Int. J. Heat Mass Transfer. Vol. 31, No. 3, pp. 603–614, 1988
Printed in Great Britain

0017–9310/88 $3.00 + 0.00
Pergamon Press plc

The gas contribution to heat transfer between fluidized beds of large particles and immersed surfaces

GERMÁN D. MAZZA and GUILLERMO F. BARRETO†
Universidad Nacional de La Plata, Centro de Investigación y Desarrollo en Procesos Catalíticos (CINDECA), Calle 47 No. 257, (1900) La Plata, Argentina

(*Received* 28 *October* 1986 *and in final form* 8 *July* 1987)

Abstract—The gas contribution to heat transfer between large particle fluidized beds and immersed surfaces is analysed through a heterogeneous model for the dense phase. An approximate solution of the governing balances provides a conceptually appropriate and precise enough expression for the gas heat transfer coefficient, h_g. For most practical conditions h_g amounts to 75–85% of the limiting heat transfer coefficient at the surface wall, h_{wg}. The results are compared with previous correlations for experimental conditions at which they were formulated. The analogous mass transfer process is included in this analysis as a particular case of the proposed theory.

1. INTRODUCTION

IT IS NOWADAYS acknowledged that heat exchange between a gas fluidized bed and immersed surfaces is carried out by three mechanisms: solid contribution due to particle convection, gas contribution and radiant heat exchange.

For small particles, say $d_p < 0.5$ mm, the solid contribution is dominant. This is usually the case for fluidized bed catalytic reactors. The assumption followed in many research works until the middle of the last decade was that the three mechanisms can be evaluated independently and efforts were focused on the modelling and correlation of the solid contribution. The gas contribution being of lesser importance, it was evaluated by assuming similarity with other processes. Some authors (e.g. Baskakov *et al.* [1] and more recently Bock [2]) evaluated the gas contribution from experiments of mass transfer between a fluidized bed and an immersed surface. This approach assumes that gas and solid phases do not exchange heat between each other and hence both phases act independently. In other studies (Xavier and Davidson [3], Denloye and Botterill [4], Barreto *et al.* [5]) the gas contribution is taken as the heat transfer rate for the same bed at minimum fluidizing conditions. The assumption in this case is that particle motion, originated by the presence of bubbles, adds its effect to that of the gas at incipient fluidization.

The process of combustion of carbonaceous materials in fluidized beds, which has been actively studied and developed since the early 1970s, has drawn attention to the evaluation of heat transfer rates in fluidized beds of large particles (1 mm in diameter or greater) and also to the operation under pressure (for the case of expanding the bed exhaust in gas turbines). The solid contribution decreases as d_p increases due to a higher thermal resistance between the immersed surface and the first layer of particles. Under these conditions particles remain approximately at the average bed temperature during the time spent in contact with the immersed surface. Simultaneously, the gas contribution increases because of greater gas velocities through the dense phase. In the case of operation under pressure it is further increased due to higher volumetric heat capacities. Thus, the gas contribution is more important than the solid contribution for d_p greater than about 1–2 mm, and it becomes dominant when fluidization is conducted under pressure.

Several investigations have been devoted to the evaluation of the gas contribution in these large particle fluidized beds. In many of them it is assumed that the resistance to heat transfer from the gas in the dense phase is localized at the wall which means that the bulk of the gas phase remains at the average bed temperature. As particles keep also at this thermal level this assumption can be interpreted as a result of a fast heat exchange between the solid and gas phases. This is rather the opposite view to that of estimating the gas contribution from mass transfer experiments. The resistance at the wall has been evaluated in different ways. For example, Glicksman and Decker [6] and Ganzha *et al.* [7] developed expressions for the gas heat transfer coefficient by assuming that most of the gas input to the bed flows through the dense phase. On the other hand, Decker and Glicksman [8] explicitly recognized the division of gas flow into dense and bubble phases and evaluated the contribution in each of them. Adams and Welty [9] developed a model for superficial gas velocities slightly in excess of U_{mf}. They solved the energy balance equation for a dis-

† Author to whom correspondence should be addressed.

NOMENCLATURE

Ar	Archimedes number, $d_p^3\rho_g(\rho_p-\rho_g)g/\mu^2$
C_g, C_p	volumetric heat capacities of gas and particles [J m^{-3} K^{-1}]
d_b	bubble diameter [m]
d_p	particle diameter [m]
d_t	tube diameter [m]
f_b	volumetric bubble fraction [dimensionless]
g	acceleration due to gravity [m s^{-2}]
H_c	heat source parameter due to interstitial gas convection, equation (13) [dimensionless]
H_p	heat source parameter due to transfer from particles, equation (13) [dimensionless]
H_r	heat source parameter due to dense phase replacement, equation (13) [dimensionless]
$\bar{h}$	bed-to-surface heat transfer coefficient [W m^{-2} K^{-1}]
h_b	bubble-phase heat transfer coefficient [W m^{-2} K^{-1}]
h_d	dense-phase heat transfer coefficient [W m^{-2} K^{-1}]
h_g, h_p	gas and particle heat transfer coefficients in the dense phase [W m^{-2} K^{-1}]
$\bar{h}_g, \bar{h}_p$	global contributions of gas and particles to $\bar{h}$, equations (4) [W m^{-2} K^{-1}]
h_{gi}, h_{pi}	gas and particle instantaneous heat transfer coefficients in the dense phase [W m^{-2} K^{-1}]
h_{pg}	gas/particle heat exchange coefficient in the dense phase [W m^{-2} K^{-1}]
h_{wg}, h_{wp}	heat transfer coefficient at the wall, for gas and particles in the dense phase [W m^{-2} K^{-1}]
k_{eg}, k_{ep}	effective thermal conductivities of gas and particles [W m^{-1} K^{-1}]
k_g	molecular gas thermal conductivity [W m^{-1} K^{-1}]
L	height of the immersed surface [m]
L_b	average distance between the top and bottom of the bubbles along the vertical axis defined by the position of the immersed surface [m]
Nu	Nusselt number (subscripts correspond to those of the specific heat transfer coefficient), hd_p/k_g [dimensionless]
Pr	Prandtl number, $C_p\nu/k_g$ [dimensionless]
P	operating pressure [Pa]
Re	Reynolds number based on superficial gas velocity, Ud_p/ν [dimensionless]
Re_d	Reynolds number in the dense phase, $U_d d_p/\nu$ [dimensionless]
Re_{mf}	Reynolds number at minimum fluidization conditions, $U_{mf}d_p/\nu$
T_f	bulk bed temperature [K]
T_w	surface wall temperature [K]
t_c	dense-phase contact time [s]
U	superficial gas velocity [m s^{-1}]
U_d	superficial gas velocity in the dense phase [m s^{-1}]
U_{mf}	superficial gas velocity at minimum fluidization conditions [m s^{-1}]
u_b	bubble rise velocity [m s^{-1}]
x	horizontal coordinate [m]
z	vertical coordinate [m].

Greek symbols

ε	dense-phase voidage [dimensionless]
ε_{mf}	bed voidage at minimum fluidization conditions [dimensionless]
ε_w	dense-phase voidage near the surface wall [dimensionless]
μ	gas viscosity [kg m^{-1} s^{-1}]
ν	kinematic gas viscosity [m^2 s^{-1}]
ρ_g, ρ_p	gas and particle densities [kg m^{-3}]
Φ	distance from distributor plate [m].

continuous boundary layer on the surface along with that for the stagnant zones around particle points of contact. The model requires numerical evaluation and the result estimates simultaneously both gas and particle resistances at the wall.

Although there may be certain operating conditions which justify an independent evaluation of heat transfer mechanisms, it is highly desirable to develop a physically sound theory describing the overall heat transfer process. As a first step to attempt the achievement of this goal we will present in this paper a model to evaluate the interaction between solid and interstitial gas in the dense phase for the case of large particles and low operating temperatures. Radiant heat exchange and temperature profiles in the solid phase can then be neglected.

The analysis of such interaction will be carried out on the basis of distinct temperature fields in the gas and solid phases and a finite heat exchange rate between them. Effective heat transfer parameters in each phase, dense phase voidage and gas interstitial velocities are assumed uniform and the restriction imposed by the immersed surface is considered via additional thermal resistances at the wall. Such a description, termed 'heterogeneous model with constant parameters', has been frequently used to describe heat transfer from the vessel wall to packed beds and was originally proposed to this end by

Olbrich [10]. It has also been acknowledged as one of the most adequate models for the analysis of packed bed reactors (e.g. De Wash and Froment [11], Pereira Duarte *et al.* [12]). To account for the transient nature of the heat exchange in the dense phase of a fluidized bed, the classical concept of packet renewal introduced by Mickley and Fairbanks [13] is used together with the heterogeneous model.

The bubble phase contribution is also discussed and evaluated to make up the overall gas contribution. The results thus obtained are discussed in the light of previous correlations.

2. ANALYSIS OF GAS CONTRIBUTION IN THE DENSE PHASE

The heat transfer rate from a gas fluidized bed to an immersed surface can be expressed as

$$q = \bar{h}(T_f - T_w) \tag{1}$$

$$\bar{h} = h_d(1-f_b) + h_b f_b \tag{2}$$

where f_b is the volumetric average bubble fraction near the surface, T_f the bulk temperature of bed and T_w the wall temperature, assumed to be uniform.

Contributions of dense and bubble phases to the overall heat transfer coefficient $\bar{h}$ are h_d and h_b, respectively. The former can be in turn split into interstitial gas and solid contributions

$$h_d = h_g + h_p. \tag{3}$$

The overall gas contribution is defined as

$$\bar{h}_g = h_g(1-f_b) + h_b f_b \tag{4a}$$

and the solid phase contribution as

$$\bar{h}_p = h_p(1-f_b). \tag{4b}$$

Therefore, $\bar{h}$ can be written alternatively as

$$\bar{h} = \bar{h}_g + \bar{h}_p. \tag{5}$$

Since heat penetration zones are normally smaller than the size of bubbles and dense phase packets, each contribution in equation (2) can be evaluated independently. On the other hand, the size of particles and of fluid elements in the dense phase can be of the order of heat penetration depths and their contributions to h_d have to be treated simultaneously. This problem will be considered next by using the heterogeneous model outlined in the Introduction. An expression for h_g will be thus developed for the case of large particles. The coefficient h_b is analysed in the next section and the overall gas contribution can finally be evaluated by means of equation (4a).

Although a simplified physical picture of the heat transfer process between the dense phase and an immersed surface will be adopted, it includes most of the variables likely to affect the heat transfer rate. Consider a vertical heat exchanging element of length L and assume that the whole surface is immersed in a dense phase packet. This is removed from the surface

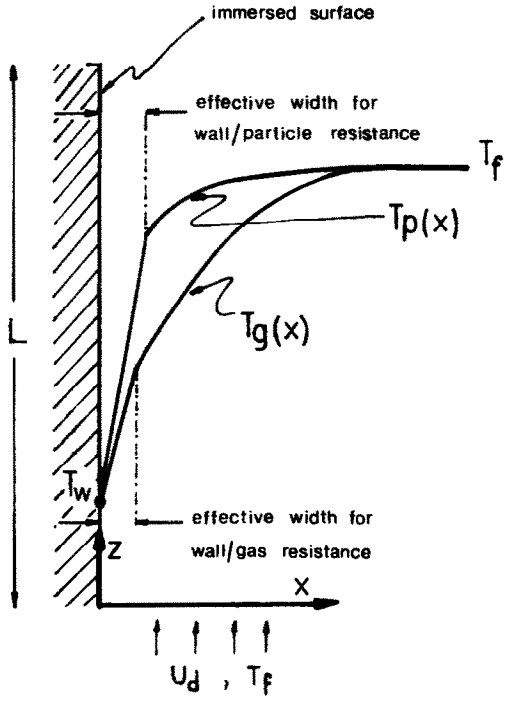

FIG. 1. Scheme of instantaneous gas and solid temperature profiles in the dense phase for a given axial position.

by the effect of bubbles passing nearby after a time interval t_c (contact time). It is further assumed that no particle movement takes place during t_c. A scheme of instantaneous temperature profiles developed in the gas and solid phases at a given axial position is given in Fig. 1. The equations governing heat transfer in the dense phase according to the heterogeneous model with constant parameters are

$$C_g(\varepsilon\,\partial T_g/\partial t + U_d\,\partial T_g/\partial z) = k_{eg}\,\partial^2 T_g/\partial x^2 + 6(1-\varepsilon)h_{pg}(T_p - T_g)/d_p \tag{6a}$$

$$C_p(1-\varepsilon)\,\partial T_p/\partial t = k_{ep}\,\partial^2 T_p/\partial x^2 - 6(1-\varepsilon)h_{pg}(T_p - T_g)/d_p \tag{6b}$$

with initial conditions given by

$$t = 0; \quad T_g = T_p = T_f. \tag{7}$$

Boundary conditions are

$$z = 0; \quad T_g = T_f \tag{8}$$

$$x = 0; \quad k_{eg}\,\partial T_g/\partial x = h_{wg}(T_g - T_w) \tag{9a}$$

$$x = 0; \quad k_{ep}\,\partial T_p/\partial x = h_{wp}(T_p - T_w) \tag{9b}$$

$$x \to \infty; \quad T_g = T_p = T_f. \tag{10}$$

The gas heat transfer coefficient is defined as

$$h_g = \int_0^L \int_0^{t_c} h_{gi}(z,t)\,dz\,dt/(Lt_c) \tag{11}$$

where h_{gi} is the instantaneous coefficient

$$h_{gi}(T_f - T_w) = k_{eg}\,\partial T_g/\partial x|_{x=0}. \tag{12}$$

Expressions analogous to equations (11) and (12) define coefficients h_p and h_{pi} for the solid phase. We will not explicitly use here the solid energy balance since for large enough particles ($d_p > 1$–2 mm) they can be assumed to be isothermal, as shown for instance by Glicksman and Decker [6] and Adams and Welty [9]. The condition $T_p = T_f$ allows us to uncouple the gas energy balance from that of the solid. A closed-form solution for the coefficient h_g (equation (11)) in this case is given in the Appendix, but a much simpler approximate expression can be obtained by following the lines of Danckwerts' penetration theory [14].

Consider that instead of a fixed value t_c, an exponential distribution holds for contact times

$$f(\tau) = \exp(-\tau/\bar{\tau})/\bar{\tau}$$

where $f(\tau)\,d\tau$ is the fraction of dense phase packets with contact times ranging from τ to $\tau+d\tau$, and $\bar{\tau}$ is the mean contact time. This distribution holds when the probability that a dense phase packet is removed from the surface is independent of the time already spent in contact. In this case, the proper definition for the gas heat transfer coefficient in the dense phase can be written as

$$h_g(\bar{\tau}) = \frac{\int_0^\infty \exp(-t/\bar{\tau}) h_{gL}(t)\,dt}{\bar{\tau}} \qquad (13)$$

where

$$h_{gL}(t) = \int_0^L h_{gi}(z, t)\,dz/L$$

$$= k_{eg} \int_0^L \left.\frac{\partial T_g}{\partial x}\right|_{x=0} dz/[L(T_w - T_f)].$$

The numerator of equation (13) can be interpreted as the Laplace transform on variable t of h_{gL} with the Laplace operator $p = 1/\bar{\tau}$. Koppel *et al.* [15] and Chen and Pei [16] used the transformed coefficients for pseudo-homogeneous models describing heat transfer between the dense phase and immersed surfaces. Assuming $\bar{\tau} = t_c$, Koppel *et al.* [15] found that their transformed coefficient was reasonably close to that corresponding to a fixed value t_c. Since expressions for the transformed coefficients are much simpler than those for fixed values of t_c, we will follow an analogous procedure, not only on variable t but on variable z as well. This is achieved by means of the following transformation:

$$\mathscr{L}(T) = \int_0^\infty \exp(-tp_t) \times \left(\int_0^\infty \exp(-zp_z) T(z, t)\,dz\right) dt.$$

Applying this double transformation to equation (6a) an ordinary differential equation in x arises. This is readily integrated and from the solution $\mathscr{L}(T_g)$ the coefficient $h_g(1/p_z, 1/p_t)$ is defined as

$$(T_f - T_w) h_g(1/p_z, 1/p_t) = p_z p_t k_{eg} \frac{\partial}{\partial x}(\mathscr{L}(T_g))|_{x=0}.$$

The result is

$$h_g(1/p_z, 1/p_t) = \frac{h_{wg}}{1 + h_{wg}/(H_p^2 + H_r^{*2} + H_c^{*2})^{0.5}} \qquad (14)$$

where

$$H_r^{*2} = k_{eg}\varepsilon C_g p_t; \quad H_c^{*2} = k_{eg} C_g U_d p_z \qquad (15)$$

$$H_p^2 = 6(1-\varepsilon) h_{pg} k_{eg}/d_p. \qquad (16)$$

Coefficient h_g may be found from the inversion of equation (14). However, the expression given in the Appendix (equation (A19)) was obtained by using previously developed formulae (Carslaw and Jaeger [17]).

The approximate equation for h_g is derived from equation (14) as follows. For large values of p_t or $p_z U_d$, $h(1/p_z, 1/p_t)/h_{wg}$ tends to $1/(1+h_{wg}/H_r^*)$ or $1/(1+h_{wg}/H_c^*)$, respectively. Similarly, for very small values of t_c or L/U_d, h_g/h_{wg} from equation (A19) tends to $1/(1+h_{wg}/H_r)$ or $1/(1+h_{wg}/H_c)$, where

$$H_r^2 = 4k_{eg}\varepsilon C_g/\pi t_c \qquad (17)$$

$$H_c^2 = 4k_{eg} C_g U_d/\pi L. \qquad (18)$$

The approximate coefficient is obtained by taking in equation (14) $p_t = 4/\pi t_c$ and $p_z = 4/\pi L$. Then

$$h_g/h_{wg} = \frac{1}{1 + h_{wg}/(H_p^2 + H_r^2 + H_c^2)^{0.5}}. \qquad (19)$$

It is worth noting that the limiting form obtained for very large H_p in equation (19) also agrees with that of equation (A19).

Differences between equation (19) and the exact expression are within approximately 5%. Since this value is lower than the precision usually achievable in heat transfer predictions we will use equation (19) for our analysis.

The meaning of the different terms in equation (19) can be readily explained. The maximum heat transfer coefficient $h_g = h_{wg}$ will be reached if the gas temperature remains at T_f. In this sense there are three mechanisms acting as heat sources for the exchanging mass of gas: the replacing mechanism by passing bubbles, the interstitial convection of gas and heat transfer from the particles. They are clearly represented by H_r, H_c and H_p, respectively, in equation (19).

In order to evaluate the relative importance of the terms in equation (19) we need expressions for the heat transfer parameters h_{wg}, k_{eg} and h_{pg}. They have been calculated from the correlations given in Table 1 which are mainly based on packed bed data, since there is a shortage of these basic parameters measured in fluidized beds. A comparison with other correlations found in the literature shows that a reasonable agreement exists at large Reynolds numbers. For $Re_d < 200$–300 differences start to become significant.

The three source terms in equation (19) are plotted

Table 1. Expressions for heat transfer and fluid-dynamic parameters used in equations (19), (23) and (24)

	Heat transfer parameters	
Yagi and Wakao [18]	$Nu_{wg} = 0.2Re_d^{0.8}\,Pr^{0.33}$; $Re_d > 40$	(T1)
Beek [19]	$Nu_{pg} = 0.6Re_d^{0.57}\,Pr^{0.33}/\varepsilon$; $50 < Re_d < 2000$	(T2)
Yagi and Kunii [20]	$k_{eg} = 0.1k_g\,Re_d\,Pr$	(T3)
Baeyens and Geldart [21]†	$Re_{mf} = -57+(57^{1/0.535}+0.0564Ar^{1/1.07})^{0.535}$	(T4)
Chen and Pei [16]	$Re_{opt}-Re_{mf} = \begin{cases}0.215Ar^{0.4} & 20 < Ar < 2\times10^4\\ 0.060Ar^{0.52} & 2\times10^4 < Ar < 10^7\end{cases}$	(T5)
	Fluid-dynamic parameters	
Baskakov *et al.* [1]	$t_c = 0.44\left[\dfrac{gd_p}{(U-U_{mf})+0.1U_{mf}}\right]^{0.14}(d_p/d_t)^{0.225}$	(T6)
Hilligardt and Werther [22] (for Geldart type D particles)	$d_b = 0.0123\{1+27(U-U_{mf})\}^{0.33}(1+6.84\Phi)^{0.5}$	(T7)
[22]	$u_b = f_b u_b + 0.71(gd_b)^{0.5}$	(T8)
From a total balance of gas	$f_b = \{b-(b^2-8U_{mf}\Delta)^{0.5}\}/2U_{mf}$	(T9)
$U_{mf}(1-f_b)+f_b u_b+3U_{mf}f_b = U$	where $b = U_{mf}+U+0.71(gd_b)^{0.5}$; $\Delta = U-U_{mf}$	
Decker and Glicksman [8]	$U_d = U_{mf}(1+2f_b)$	(T10)
	$\varepsilon = \varepsilon_{mf}$	(T11)

† Approximate expression written explicitly in Re_{mf}.

in Fig. 2 for $0.1 < t_c < 1$ s and $0.01 < L < 1$ m. The range of t_c covers the values normally found in practice. The lower value of L applies to small diameter horizontal tubes and the upper limit accounts for industrial vertical tubes. It is shown in Fig. 2 that the dominant term is that of heat transfer from the solid and the ratio H_p/h_{wg} is a weak function of Re_d, and hence it is almost independent of particle diameter. For the correlations in Table 1

$$H_p/h_{wg} = 3\left(\frac{1-\varepsilon}{\varepsilon}\right)^{0.5} Pr^{0.33}\Big/ Re_d^{0.015}.$$

The renewal term H_r is of lesser importance and the gas convection term H_c becomes significant at large values of d_p and small values of L.

Values of h_g/h_{wg} are given in Table 2. It can be observed that in spite of the wide range of values for the different parameters the ratio shows little variations. Under a given pressure level the maximum difference is 10%. A comparison for the two pressure levels, 0.1 and 8 MPa, also shows a very modest effect of this variable.

The main conclusion drawn from the data in Table 2 is that for any set of parameters, h_g is markedly dependent upon h_{wg}, although consistently smaller than this by about 15–25%. For particle diameters less than 1–2 mm this percentage will be even greater because of temperature profiles in the solid phase. It is also worthwhile recalling the insensitivity of the ratio h_g/h_{wg} to certain parameters the estimations of which cannot be achieved quite accurately, like t_c or heat transport parameters at low Re_d. As the effect of H_c is also relatively small, equation (19) derived for vertical surfaces most probably can be applied for horizontal tubes by taking $L = d_t$.

The process of mass transfer from an immersed surface can also be analysed under the model developed in this section. Assuming that particles do not adsorb the transferred component there is no exchange of mass between them and the gas or immersed surface. We recall that when heat and mass transfer processes are analogous, dimensionless

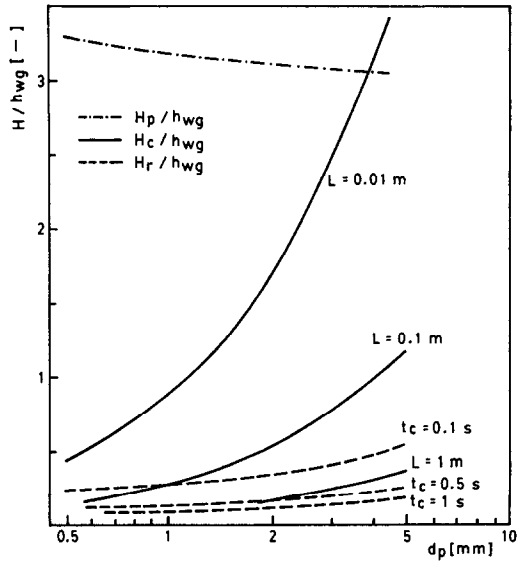

FIG. 2. Values of source terms H_r, H_c and H_p for air at room temperature and $P = 0.1$ MPa. Other parameters are: $\varepsilon = \varepsilon_{mf} = 0.4$, $\rho_p = 2000$ kg m^{-3}, $U_d = U_{mf}$ (estimated by equation (T4) in Table 1).

Table 2. Ratio h_g/h_{wg} according to equation (19) for extreme values of different parameters

(h_g/h_{wg})		$L = 0.01$ m, $t_c = 0.1$ s	$L = 0.01$ m, $t_c = 1$ s	$L = 1$ m, $t_c = 0.1$ s	$L = 1$ m, $t_c = 1$ s
$P = 0.1$ MPa	$d_p = 0.5$ mm	0.77	0.77	0.77	0.77
	$d_p = 5$ mm	0.83	0.83	0.76	0.75
$P = 8.1$ MPa	$d_p = 0.5$ mm	0.77	0.76	0.76	0.76
	$d_p = 5$ mm	0.88	0.87	0.80	0.76

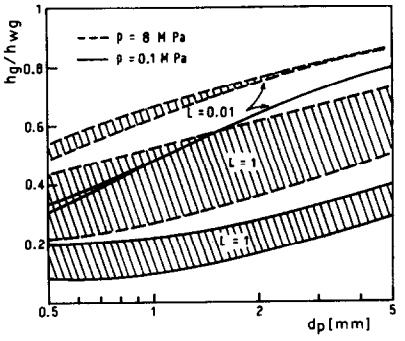

FIG. 3. Values of the ratio h_g/h_{wg} at mass transfer conditions (equation (19) with $H_p = 0$), showing the effect of d_p, P, L and t_c. Striped zones cover the range of contact times from $t_c = 0.1$ s (upper boundary) to $t_c = 1$ s (lower boundary).

expressions for transport properties are easily interchanged by using Schmidt number instead of Prandtl number and Nusselt number for mass transfer instead of Nusselt number for heat transfer. We will use throughout this work only the expressions for heat transfer. The appropriate expression for the mass transfer coefficient expressed in terms of the analogous heat transfer coefficient is obtained from equation (19) with $H_p = 0$.

Equation (19) with $H_p = 0$ is plotted in Fig. 3 as a function of d_p for different values of t_c, L and P. Other parameters were chosen as for Fig. 2. It is observed that the ratio h_g/h_{wg} becomes more sensitive to different variables than in the case of heat transfer. This is a consequence of the absence of the buffer effect provided by the source term H_p. The ratio h_g/h_{wg} in Fig. 3 only reaches values similar to those in Table 2 for small L and large d_p.

3. ANALYSIS OF BUBBLE PHASE CONTRIBUTION

In order to develop an expression for h_b the approach of Decker and Glicksman [8] is chosen as the starting point. Using Polhausen's solution [23] for heat transfer in a laminar boundary layer on a flat plate they wrote

$$h_b = 0.664 k_g \left(\frac{u}{Lv}\right)^{0.5} Pr^{0.33} \qquad (20)$$

where u is the approaching linear velocity of the gas flow. For the case of the bubble phase u is taken as the average gas velocity inside the void, which is given by $u_b + 3U_{mf}$ according to Davidson and Harrison [24]. The last term accounts for the gas 'through flow'. Equation (20) is adequate for short surfaces, but in the case of large values of L it implies that gas elements inside the bubbles exchange heat along the whole surface. This is not correct since the amount of gas entering the void through the bubble bottom will be at a temperature close to T_f and will exchange heat with the immersed surface for the period of time elapsed to reach the bubble front which will be of the order of $L_b/3U_{mf}$, L_b being the average distance between the top and bottom of bubbles along the vertical axis defined by the position of the immersed surface. Provided that L is large enough, end effects will not be important and the bubble contribution can be evaluated from equation (20) by substituting u/L by $3U_{mf}/L_b$.

An expression for all values of L can be obtained by following an analysis similar to that made by Barreto *et al.* [25] for the solid contribution to heat transfer in slugging fluidized beds. The result for the present case is

$$h_b = 0.664 k_g (\theta/\nu)^{0.5} Pr^{0.33} \qquad (21)$$

where

$$\theta = t_{mi}\{t_{ma}/(t_{ma} + t_{mi}/3)\}^2$$

$$t_{mi} = \min\{L/(3U_{mf} + u_b),\quad L_b/3U_{mf}\}$$

$$t_{ma} = \max\{L/(3U_{mf} + u_b),\quad L_b/3U_{mf}\}.$$

A simpler approximate expression is given by

$$h_b = 0.664 k_g \{(3U_{mf} + u_b)/L + 3U_{mf}/L_b\}^{0.5} \nu^{-0.5} Pr^{0.33} \qquad (22)$$

the maximum difference of which with equation (25) is 6% when $t_{mi} = t_{ma}$. The value of L_b should be the average calculated from all possible configurations of contact between a bubble and the immersed surface. We will use the result for a spherical bubble

$$L_b = 9d_b/16.$$

To the authors' knowledge there have been no experimental attempts to isolate the effect of heat or mass transfer from bubbles to immersed surfaces, although it is worthwhile to recall the analysis made by Chandran and Chen [26]. They evaluated h_b from experimental values of $\bar{h}$ by subtracting the solid and gas contributions in the dense phase. It was found that values of h_b were, in general, several times greater

than those estimated by assuming that bubbles are devoid of particles. The effect was attributed to particles raining inside the bubbles which would distort the velocity field of the gas stream improving the heat transfer efficiency. However, Chandran and Chen estimated h_g from an expression proposed by them, which in our opinion underpredicts significantly this contribution and, hence, causes too high estimates of h_b.

We believe that the presence of particles inside bubbles should enhance h_b, but not to the extent suggested by Chandran and Chen. In fact, the experiments of heat transfer from slugs to the dense phase carried out by Stubington [27] showed that the presence of particles increases heat transfer up to around 70%. This figure represents a much more modest effect than that estimated by Chandran and Chen [26]. Although both processes, heat transfer from bubbles to the dense phase and from bubbles to an immersed surface, are not strictly comparable, they present common mechanisms and it cannot be expected that the effect of particles will differ significantly in each case.

In view of the lack of more precise knowledge of the effect of particles on h_b, we will use in the next section equation (22) in addition to equation (19) to evaluate $\bar{h}_g$

$$\bar{h}_g = \frac{(1-f_b)}{\dfrac{1}{h_{wg}} + \dfrac{1}{(H_p^2+H_r^2+H_c^2)^{0.5}}} + \frac{0.664 k_g f_b\, Pr^{0.33}}{\nu^{0.5}} \times \left(\frac{3U_{mf}+u_b}{L} + \frac{3U_{mf}}{L_b}\right)^{0.5}. \quad (23)$$

4. COMPARISON OF EQUATION (23) WITH PREVIOUS CORRELATIONS

Baskakov *et al.* [1] correlated mass transfer coefficients obtained by Baskakov and Suprun [28] (naphthalene transfer from immersed vertical objects to air fluidized beds) and by Ziegler and Brazelton [29] (water transfer from spheres to fluidized beds of small particles). Their correlation expressed in terms of analogous heat transfer parameters is given by

$$\overline{Nu}_g = \begin{cases} \overline{Nu}_{g,max} = 0.009 Ar^{0.5} Pr^{0.33}; & U > U_{opt} \quad (24a) \\ \overline{Nu}_{g,max}(U/U_{opt})^{0.3}; & U < U_{opt} \quad (24b) \end{cases}$$

where U_{opt} is the superficial gas velocity at which the maximum heat transfer coefficient $\bar{h}_{max}$ is reached. It will be estimated here for equation (T5) given in Table 1.

Baskakov *et al.* [1] suggested that equations (24) can also be used to assess the gas contribution to heat transfer. As discussed in Section 2, the basic difference between mass transfer and the gas contribution for heat transfer is that there is no exchange of mass between gas and particles in the dense phase. In terms of equation (23) this difference is accounted for by the source term H_p. We will first compare equations (24) with our appropriate expression for mass transfer conditions (equation (23) with $H_p = 0$) and the use of equations (24) for heat transfer will be discussed later on.

The comparison between equation (23) with $H_p = 0$ and equations (24) have been made for the experimental conditions in the works of Baskakov and Suprun [28] and Ziegler and Brazelton [29]. Since many data correspond to small particles, values of Re_d are about unity or less. Correlations given in Table 1 for h_{wg} and k_{eg} are not valid for these small values of Re_d and they should be modified. For k_{eg}, the molecular contribution estimated as εk_g, will be added to the flow contribution in equation (T3). When heat transfer is controlled by molecular conductivity, the additional thermal resistance at the surface wall is no longer meaningful; h_{wg} should tend to infinity while h_{wg} from equation (14) tends to zero as $Re_d \to 0$. To avoid this incompatibility we modify equation (14) as

$$Nu_{wg} = 0.2 Re_d^{0.8} Pr^{0.33} + 2$$

which predicts a maximum heat transfer resistance of $d_p/2$ wide stagnant gas film as $Re_d \to 0$. Although h_{wg} is still finite, it can be shown that $1/h_{wg}$ is negligible with respect to the other term in the denominator of equation (23) as $Re_d \to 0$. Values of t_c, d_b, u_b, f_b, U_d and ε to apply equation (23) for given experimental conditions (gas and particles properties and superficial gas velocity) have been evaluated from the expressions given in Table 1. The expression for U_d deserves a brief comment. Assuming that $\varepsilon = \varepsilon_{mf}$, the average superficial velocity in the dense phase should be $U_d = U_{mf}$. Nonetheless, expression (T10) is adopted here to account for horizontal components of gas velocity in the dense phase originated by the presence of bubbles, which should contribute to gas convection in the heat (or mass) transfer process.

The most significant differences between experimental conditions in the works of Baskakov and Suprun [28] and Ziegler and Brazelton [29] are the values of L and Pr: $L = 100$ mm (average for the vertical naphthalene cylinders), $Pr = 2.6$ in ref. [28] and $L = d_{sphere} = 12.5$ mm, $Pr = 0.6$ in ref. [29]. Values of $\bar{h}_g$ from equation (23) (with $H_p = 0$) and equations (24) for both sets of (L, Pr) and different d_p are given as a function of $U - U_{mf}$ in Fig. 4. It is shown that in general the agreement is good, and it improves markedly as d_p increases ($d_p > 1$ mm). For small values of d_p, values from equation (23) are lower, which can be due in part to the uncertainty in calculating h_{wg} and k_{eg} at low Re_d. Another reason for this difference may be the probable low estimate of h_b, as discussed in Section 2, since according to equations (24) as d_p decreases $f_b h_b$ gains in importance with respect to $(1-f_b)h_g$.

With regard to the effects of L and Pr, it should be noted that equations (24) do not include the influence of L, which was found in Section 2 to be significant

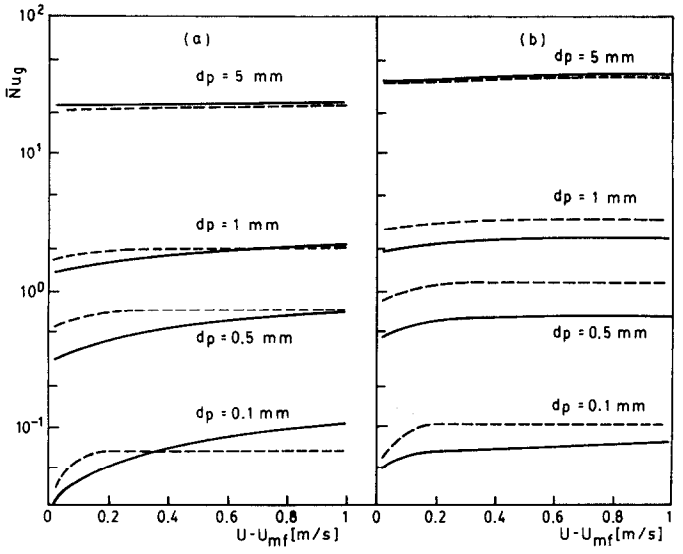

FIG. 4. Values of $\overline{Nu}_g$ for mass transfer conditions. Continuous curves are from equation (23) with $H_p = 0$, and dashed curves are from equations (24). Fluid-mechanical properties of air at room temperature are assumed, $\rho_p = 2000$ kg m^{-3}, $P = 0.1$ MPa, $\varepsilon = \varepsilon_{mf} = 0.4$, $\Phi = 0.2$ m. (a) $Pr = 0.6$, $L = 0.0125$ m, $d_t = 0.0125$ m. (b) $Pr = 2.6$, $L = 0.1$ m, $d_t = 0.03$ m.

for mass transfer conditions. In equations (24) $\bar{h}_g$ is proportional to $Pr^{0.33}$, while $\bar{h}_g$ from equation (23) increases as Pr^{α}, with an effective value of α close to 0.5 for conditions in Fig. 4. Both, L and Pr are smaller for the data in ref. [28] than those in ref. [29], and according to equation (23) their effects are roughly counterbalanced. On the other hand, equations (24) relatively underestimate the effect of Pr and ignore that of L, and therefore behave much in the same way as equation (23) for these two particular sets of data. This probably explains why Baskakov *et al.* [1] could correlate together the data of refs. [28, 29] without considering the different values of L. It is interesting to note that Ziegler and Holmes [30] presented data of naphthalene transfer from vertical plates of different lengths. An inspection of their Table 2 shows that the mass transfer rate increases as L decreases. This finding qualitatively supports the present analysis, although a numerical comparison seems unworthy since Ziegler and Holmes [30] suspected that their data were probably affected by some adsorption of naphthalene on the particles.

The experiments of Borodulya *et al.* [31, 32] are appropriate to compare equation (23) with heat transfer data. They investigated fluidized beds of large particles under pressure, conditions at which the gas contribution is dominant. This contribution was estimated in those works by the correlation of Ganzha *et al.* [7]

$$\overline{Nu}_g = 0.12 Re^{0.8} Pr^{0.43} (1-\varepsilon_w)^{0.133} \varepsilon_w^{-0.8} \quad (25)$$

where the voidage near the wall ε_w is in turn calculated from an empirical expression as a function of Re, Re_{mf}, Ar and d_p/d_t. Equation (25) was developed on the basis of a gas boundary layer on the immersed surface discontinued by the presence of particles. The factor 0.12 was found by fitting equation (25) to experimental data. The bubble contribution is not explicitly included and the Reynolds number is based on the superficial velocity U. Hence, equation (25) can be thought as being the description of heat transfer for particulate rather than aggregative fluidization. Most of the experimental data of Borodulya *et al.* [31, 32] lay within 20% of values calculated on the basis of equation (25). Therefore, equations (23) and (25) will be compared for such experimental conditions.

The gas contribution $\bar{h}_g$ is represented in Fig. 5 for the largest particles (glass ballotini, $\rho_p = 2630$ kg m^{-3}, $d_p = 1.25$ and 3.1 mm) used in ref. [32] at different pressure levels. The geometrical parameters were $\Phi = 0.07$ m and $L = d_t = 0.013$ m (corresponding to horizontal tube bundles). It can be observed that curves from equation (25) are discontinued beyond a certain value of U. This was done because the correlation for ε_w used by Ganzha *et al.* [7] predicts values near unity making the coefficient $\bar{h}_g$ drop abruptly, which is physically unsound. However, the experimental data were obtained at gas flow rates below these critical values of U.

Values of $\bar{h}_g$ predicted by equation (23) are slightly smaller than those given by equation (25); maximum differences being less than 10%. Therefore, the agreement between both expressions can be considered as being quite good.

For conditions in Fig. 5, the contribution of gas in the dense phase is, according to equation (23), definitely larger than that of the bubble phase. Therefore, any deficiency in the behaviour of equation (23) should be attributed to the evaluation of h_g. In this sense, a major uncertainty for the particular experimental conditions in refs. [31, 32] is due to the estimation of U_d, since heat transfer rates were measured

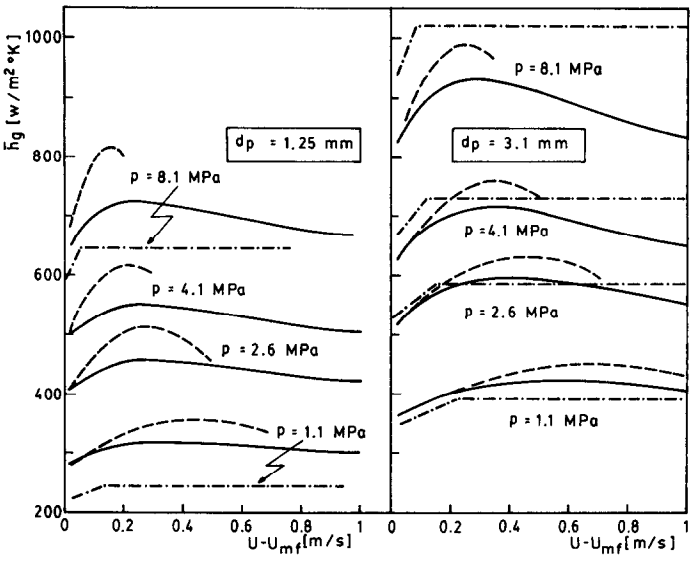

FIG. 5. Comparison of $\bar{h}_g$ according to different expressions: ——, equation (23); ----, equation (25); —·—·—·—, equations (24). Air properties at room temperature and $\varepsilon = \varepsilon_{mf} = 0.4$ are assumed.

at short distances from the distributor plate (< 100 mm), zone in which the bubble flow is not fully developed (see e.g. Hilligardt and Werther [22]) and consequently, the interstitial velocity U_d can be somewhat higher than that estimated via equation (T10) in Table 1.

Equations (24) are also plotted in Fig. 5. It can be observed that this correlation provides very good estimates for the case of the largest particles, $d_p = 3.1$ mm, but values for $d_p = 1.25$ mm are significantly lower than those from equations (23) and (25). This effect can be interpreted with the aid of the analysis made in Section 2 and recalling the very good agreement between equation (23) (with $H_p = 0$) and equations (24). As discussed before, mass transfer data on which equations (24) are based lack the particle source contribution represented by H_p in our model. For large d_p, it was shown that H_r and H_c may be large enough (Fig. 2) to lessen the effect of H_p and values of h_g/h_{wg} become similar for both mass and heat transfer processes (compare values for $d_p > 3$ mm and $L = 0.01$ m in Fig. 3 with those given in Table 2). As d_p decreases the lack of H_p is noticeable and h_g/h_{wg} becomes significantly smaller for mass than for heat transfer.

5. CONCLUSIONS

The global gas contribution to heat transfer between a fluidized bed and immersed surfaces has been evaluated by adding the individual contribution of interstitial gas in the dense phase and that of the bubble phase.

To analyse the former, a heterogeneous model with different temperature fields in gas and solid phases is proposed and the case of large isothermal particles was specifically undertaken. An exact analytical solution is found for the relatively simple geometrical configuration adopted here, but an approximate expression, based on the Laplace transform temperature field, is shown to be simpler, conceptually appropriate and precise enough to be used for practical purposes.

Numerical results for a wide range of operation conditions found in fluidization practice show that the largest heat transfer resistance is that at the surface wall ($1/h_{wg}$), but thermal penetration depths are enough to make values of the gas heat transfer coefficient in the dense phase, h_g, reach only 75–85% of h_{wg}. Therefore, a precise evaluation of h_{wg} is most important to obtain good predictions of h_g, but the influence of other thermophysical and fluid-dynamic parameters should also be taken into consideration.

The similar mass transfer problem can be interpreted as a particular case of the analysis for heat transfer.

The model was compared with previous correlations for both processes, heat and mass exchange, in particular for the experimental conditions at which the correlations were checked or developed. The agreement was in general quite satisfactory, and in addition it was shown that the full analogy between mass and heat transfer processes may hold for large particle systems ($d_p > 2$–3 mm). This provides some support for theories (e.g. refs. [1, 2]) which evaluate the global gas contribution from mass transfer correlations.

The basic heat transfer parameters used for the heterogeneous model were evaluated from correlations mainly based on packed bed data. The results presented in this paper indicate their adequacy to describe fluidized bed/immersed surface heat transfer.

REFERENCES

1. A. P. Baskakov, B. V. Berg, O. K. Vitt, N. F. Filippovsky, V. A. Kirakosyan, J. M. Goldobin and V. K. Maskaev, Heat transfer to objects immersed in fluidized beds, *Powder Technol.* **8,** 273–282 (1973).
2. H. J. Bock, Heat transfer in fluidized beds, Preprints 4th Int. Conf. on Fluidization, Kashikojima, Japan, pp. 5.2.1–5.2.8 (1983).
3. A. M. Xavier and J. F. Davidson, Heat transfer to surfaces immersed in fluidised beds, particularly tube arrays. In *Fluidization* (Edited by J. F. Davidson and D. L. Keairns), pp. 333–338. Cambridge University Press, Cambridge (1978).
4. A. O. O. Denloye and J. M. Botterill, Bed to surface heat transfer in a fluidized bed of large particles, *Powder Technol.* **19,** 197–203 (1978).
5. G. F. Barreto, A. Lancia and G. Volpicelli, Heat transfer and fluid dynamic characteristics of gas fluidized beds under pressure, *Powder Technol.* **46,** 155 (1986).
6. L. R. Glicksman and N. Decker, Heat transfer in fluidized beds with large particles, *Proc. 6th Int. Conf. on Fluidized Bed Combustion, Technical Sessions*, Vol. III, pp. 1152–1158, Atlanta, Georgia (1980).
7. V. L. Ganzha, S. N. Upadhyay and S. C. Saxena, A mechanistic theory for heat transfer between fluidized beds of large particles and immersed surfaces, *Int. J. Heat Mass Transfer* **25,** 1531–1540 (1982).
8. N. Decker and L. R. Glicksman, Heat transfer in large particle fluidized beds, *Int. J. Heat Mass Transfer* **26,** 1307–1320 (1983).
9. R. L. Adams and J. R. Welty, A gas convection model of heat transfer in large particle fluidized beds, *A.I.Ch.E. Jl* **25,** 395–405 (1979).
10. W. E. Olbrich, A two phase diffusional model to describe heat transfer processes in a non adiabatic packed tubular bed, *Proc. Chemeca '70 Conf.*, pp. 101–119. Butterworths, London (1970).
11. A. P. De Wash and G. F. Froment, A two dimensional heterogeneous model for fixed bed catalytic reactors, *Chem. Engng Sci.* **26,** 629–634 (1972).
12. S. I. Pereira Duarte, G. F. Barreto and N. O. Lemcoff, Comparison of two dimensional models of fixed bed catalytic reactors, *Chem. Engng Sci.* **39,** 1017–1024 (1984).
13. H. S. Mickley and D. F. Fairbanks, Mechanism of heat transfer to fluidized beds, *A.I.Ch.E. Jl* **1,** 374–384 (1955).
14. P. Danckwerts, Significance of liquid film coefficient in gas absorption, *Ind. Engng Chem.* **43,** 1460–1467 (1951).
15. L. B. Koppel, R. D. Patel and J. T. Holmes, Statistical models for surface renewal in heat and mass transfer. Part IV: wall to fluidized bed heat transfer coefficients, *A.I.Ch.E. Jl* **16,** 464–471 (1970).
16. P. Chen and D. C. T. Pei, A model of heat transfer between fluidized beds and immersed surfaces, *Int. J. Heat Mass Transfer* **28,** 675–682 (1985).
17. H. S. Carslaw and J. C. Jaeger, *Conduction of Heat in Solids*. Oxford University Press, London (1959).
18. S. Yagi and N. Wakao, Heat and mass transfer from wall to fluid in packed beds, *A.I.Ch.E. Jl* **5,** 79–85 (1959).
19. W. J. Beek, Mass transfer in fluidized beds. In *Fluidization* (Edited by J. F. Davidson and D. Harrison), p. 121. Academic Press, London (1970).
20. S. Yagi and D. Kunii, Studies on effective thermal conductivities in packed beds, *A.I.Ch.E. Jl* **3,** 373–381 (1957).
21. J. Baeyens and D. Geldart, Predictive calculations of flow parameters in gas fluidized beds and fluidization behaviour of various powders, *Proc. Int. Symp. Fluidization and its Applications*, p. 263, Ste. Chimie Industrielle, Toulouse (1974).
22. K. Hilligardt and J. Werther, Local bubble hold-up and expansion of gas/solid-fluidized beds, *Chemie-Ingr-Tech.* **57,** 622 (1985).
23. W. M. Kays, *Convective Heat and Mass Transfer*. McGraw-Hill, New York (1966).
24. J. F. Davidson and D. Harrison, *Fluidised Particles*. Cambridge University Press, Cambridge (1963).
25. G. F. Barreto, G. Donzi, A. Lancia and G. Volpicelli, Modelling of heat transfer between a slugging fluidizing bed and immersed vertical probes, *Powder Technol.* **41,** 41–48 (1985).
26. R. Chandran and J. C. Chen, A heat transfer model for tubes immersed in gas fluidized beds, *A.I.Ch.E. Jl* **31,** 244–252 (1985).
27. J. F. Stubington, Heat transfer between a freely-rising slug and a fluidised bed, *Trans. Instn Chem. Engrs* **58,** 195–202 (1980).
28. A. M. Baskakov and V. M. Suprun, Determination of the convective component of the heat-transfer coefficient to a gas in a fluidized bed, *Int. Chem. Engng* **12,** 324–326 (1972).
29. E. N. Ziegler and W. T. Brazelton, Mechanism of heat transfer to a fixed surface in a fluidized bed, *Ind. Engng Chem. Fundam.* **3,** 94–98 (1964).
30. E. N. Ziegler and J. T. Holmes, Mass transfer from fixed surfaces to gas fluidized beds, *Chem. Engng Sci.* **21,** 117–122 (1966).
31. V. A. Borodulya, V. L. Ganzha, A. I. Podberezsky, S. N. Upadhyay and S. C. Saxena, Heat transfer between fluidized beds of large particles and horizontal tubes bundles at high pressure, *Int. J. Heat Mass Transfer* **27,** 1219–1225 (1984).
32. V. A. Borodulya, V. L. Ganzha, A. I. Podberezsky, S. N. Upadhyay and S. C. Saxena, High pressure heat transfer investigations for fluidized beds of large particle and immersed vertical tubes bundles, *Int. J. Heat Mass Transfer* **26,** 1577–1584 (1983).

APPENDIX

Solution of energy balances in the dense phase

Provided that particles remain isothermal during t_c, $T_p = T_f$, the energy balance for the gas, equation (6) and its initial and boundary conditions, equations (7)–(10), can be written as

$$\partial\theta/\partial t + u_d\,\partial\theta/\partial z = K\,\partial^2\theta/\partial x^2 - H\theta \tag{A1}$$

$$\theta = 0 \quad \text{for } t = 0 \tag{A2}$$

$$\theta = 0 \quad \text{for } z = 0 \tag{A3}$$

$$\begin{aligned} \partial\theta/\partial x &= B_w(\theta - 1) \quad \text{for } x = 0 \\ \theta &= 0 \qquad\qquad\ \text{for } x \to \infty \end{aligned} \tag{A4}$$

where

$$\begin{aligned} \theta &= (T_g - T_f)/(T_w - T_f) \\ u_d &= U_d/\varepsilon \end{aligned} \tag{A5}$$

$$K = k_{eg}/C_g\varepsilon; \quad H = 6(1-\varepsilon)h_{pg}/C_g\varepsilon; \quad B_w = h_{wg}/k_{eg}.$$

In respect of variables z and t equation (A1) is of hyperbolic type. The characteristic equations expressed as a function of λ are

$$z_0 = u_d\lambda \tag{A6}$$

$$t = \lambda \tag{A7}$$

$$\partial\theta/\partial\lambda = K\,\partial^2\theta/\partial x^2 - H\theta. \tag{A8}$$

Equation (A8) is subject to boundary conditions (A4) for x, and initial condition

$$\theta = 0 \quad \text{for } \lambda = 0. \tag{A9}$$

Assume that the solution of equation (A8) is known, $\theta(x, \lambda)$, from which the instantaneous heat transfer coefficient can be found

$$h_i(\lambda) = h_{wg}(\theta(0,\lambda)-1) = k_{cg}\left.\frac{\partial\theta}{\partial x}\right|_{x=0}.$$

Two cases can be considered.

(a) For a given value of λ, z_0 from equation (A6) is less than L. In this case h_i and temperature profiles in x will be uniform in $z_0 < z < L$. The total heat exchanged per unit time and unit surface width in this region will be

$$q'_1 = (L-z_0)h_i(z_0/u_d). \tag{A10}$$

In the zone $0 < z < z_0$ the age of gas elements will vary from 0 to $z_0/u_d = \lambda$. Then

$$q'_2 = \int_0^{z_0} h_i(\lambda)\,dx = u_d\int_0^{z_0/u_d} h_i(\lambda)\,d\lambda. \tag{A11}$$

The total rate of heat transfer will be $q'_1+q'_2$

$$q'_1+q'_2 = q' = u_d\int_0^{z_0/u_d} h_i(\lambda)\,d\lambda+(L-z_0)h_i(z_0/u_d). \tag{A12}$$

(b) From equation (A6) z_0 is larger than L. In this case equation (A11) with the upper integration limit L/u_d applies for q'

$$q' = \int_0^{L/u_d} h_i(\lambda)\,d\lambda. \tag{A13}$$

In order to develop an expression for the average heat transfer coefficient over both $0 < z < L$ and $0 < t < t_c$, the maximum possible value of λ from equation (A7) is considered: $\lambda_{max} = t_c$. Consequently, from equation (A6)

$$z_{0,max} = u_d t_c. \tag{A14}$$

To calculate the total amount of heat exchanged during t_c per unit surface width, q'', two cases should again be considered.

Case 1: $z_{0,max} \leqslant L$. From equation (A6) we can express $z_0 = u_d t$, and integrate equation (A12) from $t = 0$ to t_c

$$q'' = \int_0^{t_c} q'\,dt = \int_0^{t_c}\left[u_d\int_0^t h_i(\lambda)\,d\lambda+(L-u_d t)h_i(t)\right]dt. \tag{A15}$$

Case 2: $z_{0,max} > L$. Now, we have to consider two steps. The first one is completed at the time $t_L = L/u_d$. The amount of heat exchanged during $0 < t < t_L$ can be found from equation (A15) by substituting t_c by t_L

$$q''_1 = \int_0^{L/u_d}\left[u_d\int_0^t h_i(\lambda)\,d\lambda+(L-u_d t)h_i(t)\right]dt. \tag{A16}$$

In the second step, defined by $t_L < t < t_c$, the temperature profile will be stationary. The amount of heat transferred is found from equation (A13)

$$q'_2 = (t_c-L/u_d)\int_0^{L/u_d} h_i(\lambda)\,d\lambda. \tag{A17}$$

Then, $q'' = q''_1+q''_2$

$$q'' = \int_0^{L/u_d}\left[u_d\int_0^t h_i(\lambda)\,d\lambda+(L-u_d t)h_i(t)\right]dt + (t_c-L/u_d)\int_0^{L/u_d} h_i(\lambda)\,d\lambda. \tag{A18}$$

The final expression for the average heat transfer coefficient will be found from

$$h_g = q''/t_c L$$

where q'' is calculated either by equation (A15) or by equation (A18). The following expression, obtained after making some algebra, unifies both cases:

$$h_g = \frac{2\int_0^{t_{mi}} t\,h(t)\,dt+t_{mi}(t_{ma}-t_{mi})h(t_{mi})}{t_{mi}t_{ma}} \tag{A19}$$

where

$$h(t_{mi}) = \frac{1}{t_{mi}}\int_0^{t_{mi}} h_i(\lambda)\,d\lambda$$

$$t_{mi} = \min(t_c, L/u_d);\quad t_{ma} = \max(t_c, L/u_d).$$

The solution of equation (A8) subject to conditions (A4) and (A9) can be found by following Carslaw and Jaeger's procedure [17] (pp. 33 and 72). The expressions needed for equation (A19) will only be given here

$$h(t_{mi}) = \frac{h_{wg}}{1-Y}[1+Y^{0.5}(I_1-1)-YI_3] \tag{A20}$$

$$\frac{1}{t_{mi}^2}\int_0^{t_{mi}} h(t)t\,dt = \frac{h_{wg}}{1-Y}\left\{0.5+Y(I_2-0.5) - \frac{Y}{\theta(1-Y)}[1-I_3+Y^{0.5}(I_1-1)]\right\} \tag{A21}$$

where

$$\theta = Ht_{mi};\quad Y = (h_{wg}/H_p)^2$$

$$I_1 = \operatorname{erfc}\theta^{0.5}-e^{-\theta}(\pi\theta)^{-0.5}+\operatorname{erf}(\theta^{0.5})/2\theta$$

$$I_2 = 0.5\left(1-\frac{1}{2\theta}\right)I_1+0.5\frac{e^{-\theta}}{(\pi\theta^3)^{0.5}}-\frac{1}{4\theta^2}\operatorname{erf}\theta^{0.5}+1/4\theta$$

$$I_3 = [1-e^{\theta(Y-1)}\operatorname{erfc}(\theta Y)^{0.5}-Y^{0.5}\operatorname{erf}\theta^{0.5}]/[\theta(1-Y)].$$

Once equations (A20) and (A21) are inserted in equation (A19), it can be observed that the ratio h_g/h_{wg} will depend on Y, Ht_c and HL/u_d, which are related to parameters in equation (19) as follows:

$$Y = (h_{wg}/H_p)^2$$

$$Ht_c = \frac{4}{\pi}(H_p/H_r)^2$$

$$HL/u_d = \frac{4}{\pi}(H_p/H_c)^2.$$

CONTRIBUTION DU GAZ AU TRANSFERT DE CHALEUR ENTRE UN LIT FLUIDISE DE GROSSES PARTICULES ET DES SURFACES IMMERGEES

Résumé—La contribution du gaz au transfert de chaleur entre un lit fluidisé de grosses particules et des surfaces immergées est analysée à l'aide d'un modèle de phase dense. Une solution approchée des bilans fournit une expression conceptuellement appropriée et suffisamment précise pour le coefficient de transfert thermique du gaz h_g. Pour des conditions plus pratiques h_g atteint 75–85% du coefficient limite de transfert à la surface h_{wg}. Les résultats sont comparés avec des relations antérieures relatives à des conditions expérimentales pour lesquelles elles ont été formulées. Le mécanisme analogue de transfert de masse est inclus dans l'analyse comme un cas particulier de la théorie proposée.

BEITRAG DER KONVEKTION ZUM GESAMTWÄRMETRANSPORT ZWISCHEN WIRBELBETTEN AUS GROSSEN TEILCHEN UND DARIN EINGETAUCHTEN OBERFLÄCHEN

Zusammenfassung—Es wird der Anteil der Konvektion auf den Wärmetransport zwischen Wirbelbetten aus großen Teilchen und darin eingetauchten Oberflächen mit Hilfe eines heterogenen Modells für die dichte Phase untersucht. Man erhält durch eine Näherungslösung der grundlegenden Bilanzgleichungen einen inhaltlich tauglichen und hinreichend genauen Ausdruck für den konvektiven Wärmeübergangskoeffizienten h_g. Für die meisten Anwendungsfälle beträgt h_g 75–85% des Wärmeübergangskoeffizienten h_{wg} an der Oberfläche der Wand. Die Ergebnisse werden mit vorhandenen Beziehungen in deren Parameterbereich verglichen. Es wird der ähnlich zu behandelnde Stofftransport als Spezialfall der vorgeschlagenen Methode vorgestellt.

ВКЛАД ГАЗА В ТЕПЛООБМЕН МЕЖДУ ПСЕВДООЖИЖЕННЫМИ СЛОЯМИ КРЧПНЫХ ЧАСТИЦ И ПОГРУЖЕННЫМИ ПОВЕРХНОСТЯМИ

Аннотация—С помощью гетерогенной модели плотной фазы анализируется вклад газа в теплообмен между псевдоожиженными слоями крупных частиц и погруженными поверхностями. Приближенное решение уравнений, определяющих равновесие, дает умозрительно подходящее и достаточно точное выражение для расчета коэффициента теплообмена газа с поверхностью, h_g. В большинстве практических случаев h_g составляет до 75–85% от общего коэффициента теплообмена слоя с поверхностью, h_{wg}. Результаты сравнивались с ранее полученными корреляциями для условий экспериментов, при которых они были получены. Аналогичный процесс массопереноса включен в этот анализ как частный случай предложенной теории.